5922 *Biochemistry* **2009,** *48,* 5922–5933
DOI: 10.1021/bi900411a

BIOCHEMISTRY
including biophysical chemistry & molecular biology
Article

Effect of Dimerization on the Stability and Catalytic Activity of Dihydrofolate Reductase from the Hyperthermophile *Thermotoga maritima*[†]

E. Joel Loveridge, Robert J. Rodriguez, Richard S. Swanwick,[‡] and Rudolf K. Allemann*

School of Chemistry, Cardiff University, Main Building, Park Place, Cardiff, CF10 3AT, United Kingdom
[‡]*Present address: Department of Life Sciences, Imperial College, London, SW7 2AZ, United Kingdom*

Received March 10, 2009; Revised Manuscript Received May 4, 2009

ABSTRACT: In contrast to all other chromosomally encoded dihydrofolate reductases characterized so far, dihydrofolate reductase (DHFR) from the hyperthermophile *Thermotoga maritima* forms a highly stable dimer. The dimer interface involves residues whose mobility is important for catalysis in monomeric DHFRs. Here, we report the generation of a variant of DHFR from *T. maritima*, TmDHFR-V11D, in which a single amino acid replacement was sufficient to favor the monomeric form of the enzyme in the presence of the nondenaturing zwitterionic detergent 3-[(3-cholamidopropyl)dimethylammonio]-1-propanesulfonate. The free energy of stabilization of monomeric TmDHFR-V11D was 15 kJ mol^{-1} lower than that of the wild-type dimer, while the melting temperature of monomeric TmDHFR-V11D was comparable to that of monomeric DHFR from the thermophile *Bacillus stearothermophilus*, supporting the hypothesis that oligomerization is required to achieve the thermal stabilities necessary for activity at temperatures optimal for growth of hyperthermophiles. Both the steady-state turnover numbers and rates of hydride transfer were reduced in TmDHFR-V11D. However, a similar reduction of the rate constants was observed in a different variant, TmDHFR-V126E, which remained as a dimer under all experimental conditions used here. Monomeric TmDHFR-V11D had a similar rate of hydride transfer to the dimeric form, but a reduced steady-state turnover rate. Intersubunit motions therefore appear to be less important than correlated motions within individual subunits for TmDHFR-catalyzed hydride transfer, but are critical to the overall progression of the catalytic cycle. Hence, the reduced catalytic activity of TmDHFR relative to the monomeric *Escherichia coli* enzyme is not caused by rigidity resulting from dimerization, but is a subtle consequence of the sequence and structure of its subunits, which appear to have evolved to allow thermostability at the expense of catalysis.

Dihydrofolate reductase (DHFR)[1] is a key enzyme during folate metabolism in eukaryotes and prokaryotes as well as in several viruses. It catalyzes the NADPH-dependent reduction of 7,8-dihydrofolate (H_2F) to 5,6,7,8-tetrahydrofolate (H_4F), which acts as a carrier of one-carbon units during the synthesis of thymidylate, purines, and several amino acids (*1*). Because of this central position in metabolism and their pharmacological importance, DHFRs from more than 30 species and all three kingdoms of life have been characterized with respect to their structure and function. Hence, DHFR has served as a paradigm for the study of the relationship between enzyme structure, dynamics, and catalysis.

DHFR from *Escherichia coli* (EcDHFR) is a monomeric enzyme consisting of four α-helices, eight β-strands, and four mobile loops (Figure 1) separated into three domains: the adenosine binding domain (ABD), the loop domain (LD), and the N-terminal domain (ND) (*2*). Previous theoretical and experimental studies have indicated the central role of several surface loops for the catalytic activity and mechanism of DHFR (*3*−*8*). The relationship between movements of these loops and catalysis has been probed by site-directed mutagenesis (*9*, *10*). Replacement of Gly121, a highly mobile residue over 19 Å from the active site and located in the middle of the βFG loop, with Val or Leu slowed the hydride transfer rate dramatically and weakened binding of NADPH (*10*). Molecular dynamics (MD) simulations of EcDHFR revealed a strong correlation between the movement of the

[†]This work was supported by the Biotechnology and Biological Sciences Research Council (BBSRC) through Grant BB/E008380/1, the University of Birmingham and Cardiff University.

*To whom correspondence should be addressed. Address: School of Chemistry, Cardiff University, Main Building, Park Place, Cardiff, CF10 3AT, United Kingdom. Phone: (44) 29 2087 9014. Fax: (44) 29 2087 4030. E-mail: allemannrk@cf.ac.uk.

[1]Abbreviations: DHFR, dihydrofolate reductase; EcDHFR, DHFR from *Escherichia coli*; TmDHFR, DHFR from *Thermotoga maritima*; BsDHFR, DHFR from *Bacillus stearothermophilus*; NADPH, nicotinamide adenine dinucleotide phosphate; H_2F, 7,8-dihydrofolate; H_4F, 5,6,7,8-tetrahydrofolate; ABD, adenosine binding domain; LD, loop domain; ND, N-terminal domain; BSA, bovine serum albumin; CHAPS, 3-[(3-cholamidopropyl)dimethylammonio]-1-propanesulfonate; MTX, methotrexate; MD, Molecular dynamics; QM/MM, quantum mechanics/molecular mechanics; KIE, kinetic isotope effect; OD, optical density; MALDI-TOF, matrix assisted laser desorption ionization - time-of-flight; CD, circular dichroism.

 Published on Web 05/19/2009

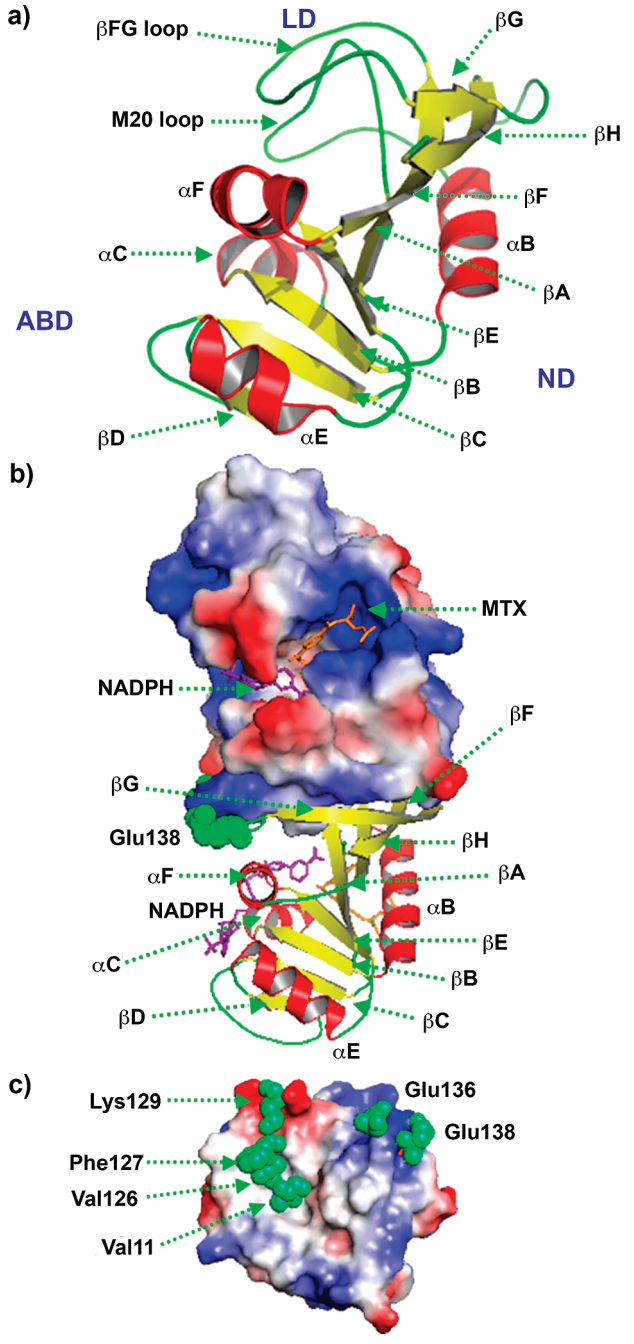

FIGURE 1: (a) Structure of EcDHFR indicating the adenosine binding domain (ABD), N-terminal domain (ND), loop domain (LD), and the flexible M20 and βFG loops (PDB 1DRE).(*2*) (b) Structure of TmDHFR bound to methotrexate and NADPH (PDB 1D1G) (*18*). One subunit is shown as a ribbon diagram, while the electrostatic potential surface calculated by PyMOL is displayed for the other. Blue and red colors indicate positive and negative potential, respectively. (c) View of the dimer interface indicating the central hydrophobic core and the more polar perimeter. Val11, Val126, Phe127, Lys129, Glu136, and Glu138 are highlighted.

catalytically important M20 and βFG loops (*11*). These correlated motions were only observed in reactive complexes of the enzyme and were absent in the product complex. Mixed quantum mechanics/molecular mechanics (QM/MM) simulations and genomic sequence analysis identified a network of hydrogen bonds and van der Waals contacts that may facilitate hydride transfer, suggesting a direct link between the motion of the βFG loop and the catalytic events in the active site of EcDHFR (*12*, *13*).

DHFR from the hyperthermopilic bacterium *Thermotoga maritima* (TmDHFR) is the most thermostable DHFR isolated so far (*14*−*16*). Its melting temperature of 83 °C is approximately 30 °C above that of EcDHFR (*17*). TmDHFR is unique among known chromosomally encoded DHFRs in that it forms a stable dimer (*16*). Like the monomeric *E. coli* enzyme, each of the two subunits of dimeric TmDHFR has three subdomains, namely, ABD, LD and ND, and despite only 27% sequence identity, the two enzymes adopt similar tertiary structures (Figure 1) (*18*). In the dimer interface of TmDHFR, a large, tightly packed and hydrophobic core around Phe127 is flanked by intermolecular ion pairs on the periphery and involves residues in the βFG loop, namely, Lys129 of one subunit and Glu136 and Glu138 of the other (Figure 1). The catalytic activity of TmDHFR is lower than that of EcDHFR even when compared at their respective physiological temperatures (*17*). The fact that residues of the βFG loop, which is critical to catalysis in EcDHFR, are involved in dimerization in TmDHFR suggests that the reduced catalytic efficiency of the thermophilic enzyme may be a consequence of the reduced mobility of this loop.

An increasing number of experimental studies of the temperature dependence of the kinetic isotope effects (KIEs) in enzyme catalyzed hydrogen transfer reactions have emphasized the role of quantum mechanical tunnelling (*19*−*31*). For TmDHFR, temperature independent KIEs were observed at elevated temperatures, while below 25 °C the KIEs became temperature dependent (*25*). These data were in good agreement with the environmentally coupled model for H-tunnelling as developed by Kuznetsov and Ulstrup (*32*) and adapted to enzymatic H-transfer by Klinman and co-workers (*33*). QM/MM calculations using ensemble-averaged variational transition state theory with multidimensional tunnelling confirmed that hydride transfer in TmDHFR occurs with a substantial contribution from quantum mechanical tunnelling (*34*).

Under no experimental circumstances has a folded TmDHFR monomer been observed, and hence a two-state unfolding reaction was proposed for TmDHFR, where the native dimer is in direct equilibrium with the unfolded monomer (*16*). It was possible however to study the hypothetical monomer in silico. MD simulations predicted the high stability of TmDHFR to result from both strong interactions between the subunits and an intrinsically increased stability of the monomeric subunits relative to the monomer of EcDHFR (*35*). QM/MM calculations revealed the presence of several of the correlated motions within individual subunits of TmDHFR that had been identified previously in EcDHFR (*12*), such as the concerted movement of the "M20" and the βFG loops (*34*). An increase of the activation energy for hydride transfer was predicted for the monomer, suggesting it would be kinetically compromised. Dimerization may therefore not only be important for stability but also for the catalytic efficiency of TmDHFR. However, the high stability of the TmDHFR dimer has so far precluded experimental verification of these predictions.

Here we report the generation and characterization of variants of TmDHFR in which hydrophobic amino acid residues in the core of the dimer interface were replaced with anionic residues. In one case such a replacement perturbed the monomer−dimer equilibrium sufficiently to allow us to address experimentally the effects of dimerization on stability and catalytic activity.

MATERIALS AND METHODS

Chemicals. All chemicals and restriction enzymes were purchased from Sigma-Aldrich, Fisher, Melford, New England

Biolabs or Fluka unless otherwise stated. Oligonucleotides were purchased from Alta Bioscience, University of Birmingham, Birmingham, UK. H_2F was prepared by dithionite reduction of folate as previously described (*17*). NADPH concentrations were determined spectrophotometrically using an extinction coefficient of 6200 cm^{-1} M^{-1} at 339 nm (*36*). Similarly, the concentration of H_2F was measured assuming an extinction coefficient of 28 000 cm^{-1} M^{-1} at 282 nm for pH 7.4 (*26*).

Site-Directed Mutagenesis. TmDHFR variants were generated using the QuikChange Site-Directed Mutagenesis Kit (Stratagene) following the manufacturer's protocol from a previously described pET-11c based expression vector harboring the gene encoding TmDHFR (*17*). Mutagenic primers were 5′-CTGTCGAACCGTACGAGTTCGGAAAGGGAATAC-3′ (V126E) and 5′-GTTCTTGCGATGGACGACTCCGGAAAGATAGCC-3′ (V11D) (changes underlined). DNA sequences were confirmed by automated DNA sequencing (Functional Genomics Laboratory, School of Biosciences, University of Birmingham, Birmingham, UK).

Protein Purification. For production of TmDHFR, TmDHFR-V11D, and TmDHFR-V126E, BL21-CodonPlus (DE3)-RP cells (Stratagene) containing the respective plasmid were grown at 37 °C in LB medium containing 200 μg/mL ampicillin to an OD_{600} of 0.6. Expression was induced by adding isopropyl-β-D-thiogalactopyranoside to a final concentration of 0.4 mM, and the culture was incubated for a further 3 h. Cells were harvested by centrifugation for 10 min at 11000*g*, and the pellet was resuspended in 50 mM Tris (pH 7.0) containing 1 mM EDTA, sonicated 5 times for 1 min on ice, treated with DNase (20 μg/mL), RNase (20 μg/mL) and $MgSO_4$ (20 mM) for 1 h at 25 °C, and centrifuged for 20 min at 27000*g*. The supernatant solution containing TmDHFR was heated to 75 °C for 20 min in a water bath and precipitated proteins separated by centrifugation for 20 min at 27000*g*. The supernatant solutions containing TmDHFR-V11D and TmDHFR-V126E were not heat treated due to their lower thermal stability. Supernatant solutions were applied to a HiPrep 16/10 SP XL cation-exchange column (GE Healthcare) and purified as described for the wild-type enzyme (*17*), leading to essentially pure proteins as judged by SDS−polyacrylamide gel electrophoresis. Masses of 19270.5 and 19258.2 were determined for TmDHFR-V11D and TmDHFR-V126E by MALDI-TOF mass spectrometry and agreed well with the calculated values of 19268.3 and 19254.0. Protein concentrations were determined spectroscopically assuming an extinction coefficient of 22 800 M^{-1} cm^{-1} at 280 nm or colorimetrically using a tannic acid based assay for the mutants (*16*).

Circular Dichroism Spectroscopy. Circular dichroism (CD) experiments were performed on an Applied Photophysics Chirascan Circular Dichroism Spectrometer using protein concentrations of 0.5 μM in 5 mM potassium phosphate (pH 7.0) in a quartz cuvette (1 cm path length, Helma) under N_2. The measured ellipticities were converted to mean residue ellipticities, $[\Theta]_{MRE}$, according to the equation: $[\Theta]_{MRE} = \Theta/(10ncl)$, where Θ is the measured ellipticity in mdeg, n is the number of backbone amide bonds, c is the concentration of protein in mol L^{-1}, and l is the path length in cm. CD unfolding measurements were obtained at 222 nm with a temperature gradient of 5 °C h^{-1} between 10 and 90 °C. Spectra were recorded for temperature steps of 0.5 or 1 °C. Where required, the enzyme was incubated with one or both of methotrexate (10 μM) and CHAPS (0.25% w/v) for 30 min prior to CD measurement. Varying the concentration of CHAPS (minimum 0.1%) did not affect the melting temperature. As had been seen for the wild-type enzyme (*17*), thermal denaturation of the mutants was irreversible. Methotrexate (MTX) was the only ligand used for thermal stability studies due to the relative instability of NADPH and H_2F at higher temperatures.

Size Exclusion Chromatography. Size exclusion chromatography was conducted to determine apparent molecular weights (M_w) using a Superdex 75 10/300 GL column (GE Healthcare) with a flow rate of 0.5 mL min^{-1}. Enzyme concentrations between 10 to 100 μM in 100 mM potassium phosphate (pH 7.0), 100 mM NaCl were used. Where required, the enzyme was incubated with one or more of NADPH (200 μM), methotrexate (200 μM), and CHAPS (0.25% w/v) for 60 min prior to injection onto the column. Varying the concentration of CHAPS (minimum 0.1%) did not affect the monomer to dimer ratio. Calibration standards were blue dextran (M_w 2×10^6; elution volume, V_e = 7.64 ± 0.13 mL; this was used to define the void volume V_o), ovalbumin (M_w 45 000; V_e = 9.28 ± 0.30 mL), EcDHFR-A79C (dimer, M_w 36 000; V_e = 9.85 ± 0.11 mL), EcDHFR-A79C (monomer, M_w 18,000; V_e = 11.49 ± 0.13 mL), EcDHFR (M_w 18,000; V_e = 11.59 ± 0.04 mL), and lysozyme (M_w 14 600; V_e=14.23 ± 0.11 mL). The EcDHFR-A79C mutant used was developed in our laboratory as a DHFR molecular weight standard, as it can be readily converted to a dimer by oxidation to form a disulfide bridge between the engineered cysteines. It is based on the double mutant EcDHFR-C85A/C152S, which has folding, stability, and kinetic properties very similar to those of the wild-type enzyme (*37*, *38*). From the elution volumes of these standards, a calibration curve was calculated: $\log M_w = 4.7457 - 0.780\,(V_e - V_o)V_o^{-1}$. Where both monomer and dimer peaks were observed, the relative areas of the two peaks were used to determine the concentrations of monomer and dimer present, and these were then used to calculate the dissociation constant (K_D) assuming a simple equilibrium between two monomers (M) and one dimer (D) ($K_D = [M]^2/[D]$). Fractions containing the monomer peak were collected and reinjected onto the column after 0.5 to 20 h incubation at 20 °C. The change in the relative areas with time was used to determine the half-life of the return to equilibrium.

Equilibrium Unfolding Measurements. To determine the free energy of stabilization, enzyme (5 μM) was incubated in 100 mM potassium phosphate (pH 7.0), 100 mM NaCl with varying concentrations of urea or guanidinium hydrochloride in the presence and absence of 0.25% CHAPS in sealed tubes for 72 h at 20 °C. Fluorescence emission was monitored using a Perkin-Elmer LS55 luminescence spectrometer (excitation at 280 nm and emission at 345 nm; slit widths 5 nm, integration time 10 s) at 20 °C. No significant change in fluorescence signal was observed after this incubation time.

The ratio of folded and unfolded protein at each denaturant concentration was calculated as described for the wild-type enzyme (*16*). The concentration of denaturant required for 50% unfolding ($C_{1/2}$) was determined by fitting the data to a sigmoidal curve using SigmaPlot 10. The folded/unfolded ratios in the transition regions were used to calculate the free energy of stabilization ΔG, and linear extrapolation to zero denaturant concentration yielded the free energy of stabilization in buffer alone (*16*).

Ligand Binding. Ligand binding was monitored in 100 mM potassium phosphate (pH 7.0), 100 mM NaCl in measurements

of the quenching of the intrinsic tryptophan fluorescence on a Perkin-Elmer LS55 luminescence spectrometer at 20 °C (excitation at 292 nm and emission at 300−550 nm; slit widths 4 nm (excitation), 10 nm (emission)). Spectra (in the presence and absence of 0.25% CHAPS) were recorded of the enzyme (4 μM) alone and in the presence of 0.5 μM increments of the ligands (to 7 μM).

Steady-State Kinetic Measurements. Turnover rates were measured spectrophotometrically by following the decrease in absorbance at 340 nm during the reaction (ε_{340} (NADPH + H_2F) = 13 200 M^{-1} cm^{-1}) (*25*). The temperature was measured from 5 to 60 °C at pH 7. The enzyme (10 μM) was preincubated at 4 °C with NADPH (20 μM) for 15−20 min to avoid hysteresis (*36*). The enzyme-NADPH solution (10 μL, final concentration 100 nM) was added to 970 μL of 100 mM potassium phosphate buffer (pH 7.0) containing 100 mM NaCl. NADPH (100 μM final concentration) was added to the solution, and the reaction was initiated by adding H_2F (100 μM final concentration). The extinction coefficient of NADPH is temperature dependent and a correction factor of −0.13% per 1 °C rise in temperature was applied for ε_{340} (*39*). Every data point is the result of nine independent measurements. The calculated k_{cat} values are based on the number of binding sites (i.e., per monomer). As there is no evidence for nonindependent behavior between subunits in the dimer, this allows direct comparison of k_{cat} values regardless of the specific monomer to dimer ratio. The k_{cat} value was unaffected by raising the protein concentration to 1 μM.

Variation of the concentrations of both substrate and cofactor showed that K_m values for all three enzymes in the presence and absence of CHAPS were below 1 μM, as had been seen for the wild-type enzyme (*17*). Accurate K_m values could not be determined due to the low reaction rates, which necessitated too high an enzyme concentration to obtain good data. All steady-state experiments reported here were therefore performed under saturating conditions. Hence, all rate constants may be considered true k_{cat} values even though only a single reagent concentration was used.

To determine the relative loss of activity with time, 25 μM TmDHFR, TmDHFR-V11D, and EcDHFR were incubated at 40 and 60 °C in the presence and absence of 0.25% CHAPS. At regular intervals, 100 μL (TmDHFR) or 16 μL (EcDHFR) aliquots were removed and added to 100 mM potassium phosphate (pH 7.0) containing 100 mM NaCl (to give 1 mL final volume). Once the temperature had stabilized at 20 °C NADPH (100 μM) was added and incubated for 5 min to avoid hysteresis, and the reaction was then initiated by adding H_2F (100 μM).

Pre-Steady-State Kinetic Measurements. Pre-steady-state kinetics experiments were performed on an Applied Photophysics stopped-flow spectrophotometer essentially as described before (*25*). Hydride transfer rates were measured following the fluorescence resonance energy transfer from the protein to NADPH in 100 mM potassium phosphate (pH 7.0) containing 100 mM NaCl. The sample was excited at 292 nm and the emission measured using an output filter with a cutoff at 400 nm. The enzyme (20 μM final concentration) was preincubated with NADPH (8 μM final concentration) in buffer for at least 15 min to avoid hysteresis. The reaction was started by rapidly mixing the enzyme−cofactor complex with H_2F (200 μM final concentration) in the same buffer. All experiments were repeated nine times. Varying the concentrations of the reagents showed that the measured rates were limiting rates for hydride transfer.

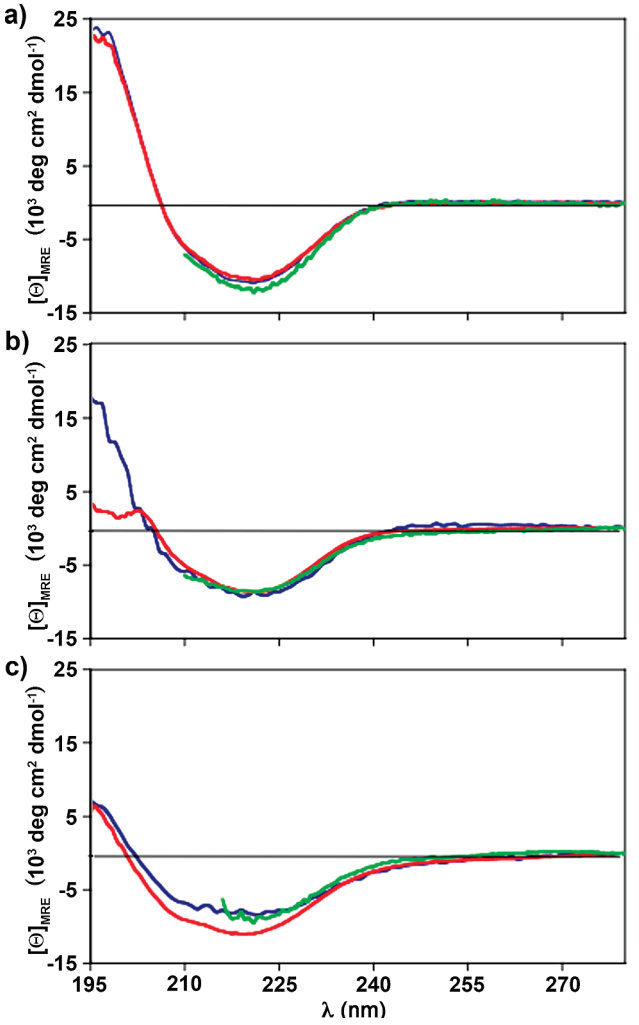

FIGURE 2: CD spectra of (a) TmDHFR, (b) TmDHFR-V126E, and (c) TmDHFR-V11D in 5 mM potassium phosphate (pH 7.0) (dark blue line), and in the presence of the inhibitor methotrexate (10 μM) (red line) or the detergent CHAPS (0.25%) (green line). Protein concentrations were 0.5 μM.

RESULTS AND DISCUSSION

Design of TmDHFR Mutants. The high stability of the TmDHFR dimer has precluded the experimental characterization of its folded monomeric subunits (*16*). As mentioned above, the hydrophobic core of the dimer interface flanked by intersubunit salt bridges and hydrogen bonds has been proposed to be the main contributor to dimer stability (*18*). A reduction in the favorable interactions within this interface should therefore lead to an increase in the concentration of folded monomer. Two spatially adjacent residues, Val11 and Val126, located toward the edge of the central hydrophobic patch next to the more hydrophilic periphery (Figure 1) were replaced with acidic residues to reduce the size of the hydrophobic core, thereby weakening the interaction between the subunits. DNAs for TmDHFR-V11D and TmDHFR-V126E were generated by site directed mutagenesis, expressed in *E. coli*, and purified as had been described previously for the wild-type enzyme (*17*).

Conformational Analysis by CD Spectroscopy. To establish the robustness of the secondary structure of TmDHFR to the replacement of residues 11 and 126, respectively, far-UV CD spectra were recorded for TmDHFR, TmDHFR-V11D, and TmDHFR-V126E. The CD spectra of all three proteins had similar shapes and shared a minimum at 222 nm at 20 °C (Figure 2).

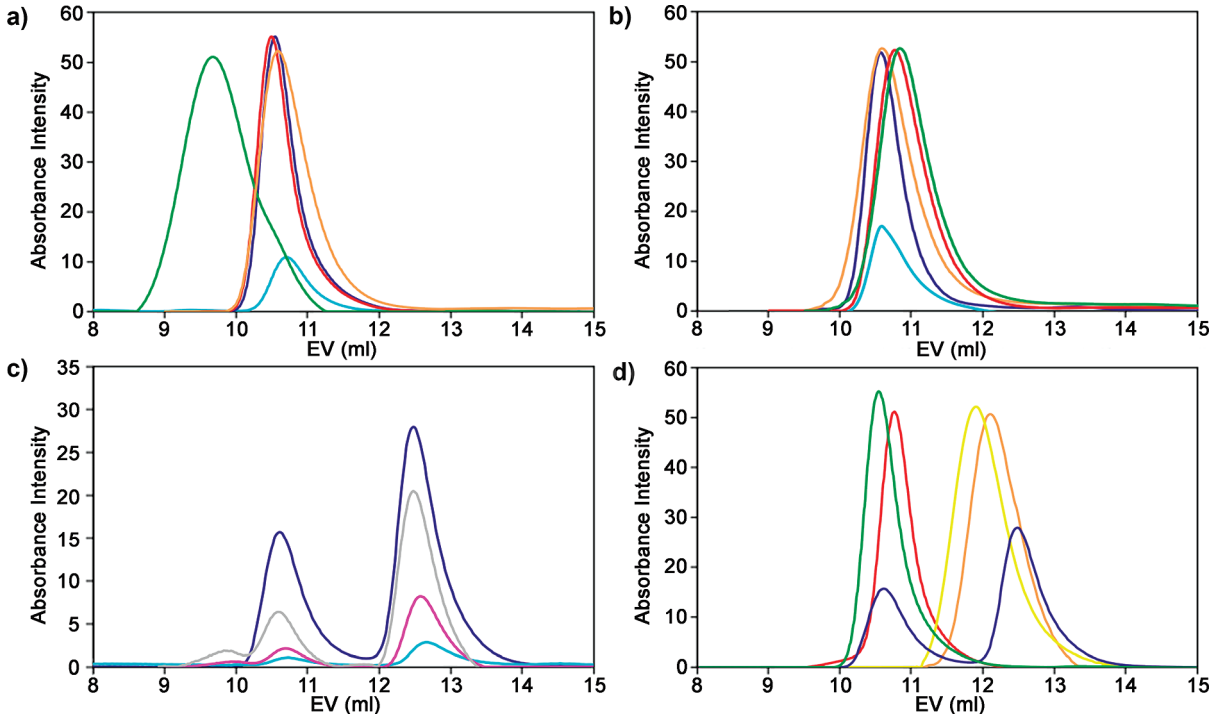

FIGURE 3: Size exclusion chromatography of TmDHFR, TmDHFR-V126E, and TmDHFR-V11D. (a) TmDHFR at 100 (dark blue line) and 10 μM (light blue line), and at 100 μM in the presence of CHAPS (orange line), MTX (red line), or NADPH and MTX (green line); (b) TmDHFR-V126E at 100 (dark blue line) and 10 μM (light blue line), and at 100 μM in the presence of CHAPS (orange line), MTX (red line), or NADPH and MTX (green line); (c) TmDHFR-V11D at 100 (dark blue line), 75 (gray line), 50 (pink line), and 10 (blue line) μM; (d) TmDHFR-V11D at 100 μM (dark blue line), and in the presence of MTX (red line), NADPH and MTX (green line), CHAPS (orange line), or CHAPS, MTX, and NADPH (yellow line).

The mean residue ellipticities, $[\Theta]_{MRE}$, at 222 nm were $-10\,727 \pm 150$, -8560 ± 144, and -8291 ± 202 deg cm^2 dmol^{-1} residue^{-1} for the wild type, TmDHFR-V126E, and TmDHFR-V11D, respectively. This suggests that amino acid replacements in the dimer interface did not lead to major changes of the secondary structures. The CD spectrum for the wild-type enzyme is in good agreement with those published previously (*17*, *40*). The zwitterionic, nondenaturing detergent 3-[(3-cholamidopropyl)dimethylammonio]-1-propanesulfonate (CHAPS) is known to destabilize intermolecular interactions. Spectra in the presence of 0.25% CHAPS were only recorded above 215 nm due to the strong absorbance of the detergent at shorter wavelengths and were found to be similar to those obtained in the absence of CHAPS (Figure 2), indicating that the detergent had only minor effects on the secondary structures of the proteins. In the presence of CHAPS, the values of $[\Theta]_{MRE}$ at 222 nm were $-11\,190 \pm 227$, -8556 ± 171, and -8389 ± 109 deg cm^2 dmol^{-1} residue^{-1} for TmDHFR, TmDHFR-V126E, and TmDHFR-V11D, respectively.

Changes in the secondary structure of TmDHFR-V11D could be observed by CD spectroscopy upon addition of ligands (Figure 2). The spectrum of the ternary complex of TmDHFR-V11D closely resembled that of the wild-type enzyme suggesting that the presence of ligands induced a structural rearrangement in TmDHFR-V11D. Only minor changes in the CD spectra of TmDHFR and TmDHFR-V126E were observed on addition of ligands.

Size Exclusion Chromatography. To determine the apparent molecular weights of the proteins under native conditions, samples of TmDHFR, TmDHFR-V11D, and TmDHFR-V126E were analyzed by size exclusion chromatography (Figure 3 and Supporting Information). From the elution volume of a 100 μM solution of TmDHFR at pH 7 an apparent molecular weight of 27900 ± 2600 was calculated by comparison with the elution volumes of molecular weight standards. Similarly, an apparent molecular weight of 27600 ± 900 was obtained for TmDHFR-V126E. 10-fold reduction of the protein concentration did not lead to a significant change in the apparent molecular weight (Figure 3A,B). The apparent molecular weight of TmDHFR was between the expected value for the monomer of 19 119 and that of the dimer. The elongated form of native TmDHFR dimer seen in the crystal structure (*18*) might be the cause for this anomalous behavior on the column. When the experiments were repeated in the presence of an excess of the inhibitor methotrexate, no change in the elution volume for the TmDHFR complex was observed. However, when both methotrexate and NADPH were present, the elution volume was reduced (Figure 3A) and indicated an apparent molecular weight of 33900 ± 800 for the ternary complex. The elution volumes measured for TmDHFR-V126E on the other hand were not significantly affected by the presence of the ligands (Figure 3B).

The elution profile for TmDHFR-V11D at 100 μM concentration showed two peaks that corresponded to apparent molecular weights of 27700 ± 2300 and 17700 ± 900 (Figure 3C). The positions of these peaks were not dependent on the concentration of TmDHFR-V11D between 10 and 100 μM. The relative peak areas however changed with the concentration of protein suggesting a slow equilibrium between the two species with an equilibrium constant of 313 ± 10 μM. Reinjection of the monomer peak fraction onto the column gave the same two peaks that had been observed originally. By determining the relative areas of the two peaks after various incubation times before reinjection, the half-life of the return to equilibrium was

estimated to be approximately 200 min. For incubation times greater than 12 h (approximately four half-lives), the monomer−dimer ratio was indistinguishable from that of the original sample. The addition of NADPH and methotrexate to TmDHFR-V11D led to the disappearance of the smaller molecular weight peak; only a single peak for a species with an apparent molecular weight of 26700 ± 1200 was observed (Figure 3D). Similarly, when TmDHFR-V11D was analyzed in the presence of methotrexate alone, only a single peak was observed corresponding to a protein of 26400 ± 1300 apparent molecular weight. This was in good agreement with the CD results reported above that had indicated a conformational change in TmDHFR-V11D on addition of the ligands. These results suggested that replacement of Val11 with aspartate destabilized the dimer sufficiently to lead to the establishment of an equilibrium in which the concentration of the monomer exceeded that of the dimer at the concentrations used, at least in the absence of the ligands. Upon addition of cofactor and substrate the dimer was stabilized and, as was the case for wild-type TmDHFR and TmDHFR-V126E, was the predominant species in solution.

To address whether CHAPS could destabilize the dimeric form of TmDHFR-V11D sufficiently to shift the equilibrium further in the direction of the monomer, size exclusion chromatography was performed in the presence of the detergent. TmDHFR-V11D eluted as a single symmetric peak of apparent molecular weight 19500 ± 500 (Figure 3D), while the detergent did not significantly alter the elution profiles of the wild type and of TmDHFR-V126E (Figure 3A,B). Even in the presence of methotrexate and NADPH, only a single species of molecular weight 20400 ± 1800 was observed for TmDHFR-V11D indicating that in the presence of CHAPS the monomeric form of TmDHFR-V11D was predominant under the conditions used for all the kinetic experiments described below.

Thermal Stability. To determine the effect of the mutations on the thermal stability of TmDHFR, the temperature dependence of the CD spectra was measured at enzyme concentrations of 0.5 μM. The denaturation curves showed midpoints at 48.2 ± 0.2 and 48.8 ± 2.4 °C for TmDHFR-V126E and TmDHFR-V11D, respectively (Figure 4 and Supporting Information), similar to the T_m of 51.6 ± 0.7 °C measured previously for EcDHFR (*41*). Under these conditions TmDHFR-V11D is predominantly monomeric, whereas TmDHFR-V126E is likely to be predominantly dimeric. In the size exclusion chromatography experiments, the dimer of TmDHFR-V11D was still detectable at concentrations as low as 10 μM (K_D = 313 μM), whereas no monomer was detectable for TmDHFR-V126E at that concentration, suggesting that the K_D for TmDHFR-V126E is below 0.5 μM. The mutations at the dimer interface therefore reduced the melting temperature of both proteins irrespective of the monomer−dimer equilibrium.

Since the size exclusion chromatography and CD experiments described above had suggested that the addition of methotrexate shifted the equilibrium toward the dimer of TmDHFR-V11D, the melting temperatures of the wild type and the two mutants were also measured in the presence of this inhibitor (Figure 4). Both TmDHFR and TmDHFR-V126E were stabilized by the presence of the ligand under otherwise identical conditions and melting temperatures of 85.2 ± 1.3 and 52.5 ± 0.4 °C were measured. While for TmDHFR and TmDHFR-V126E the shapes of the melting curves were not altered by the addition of the ligand, the melting curve of the methotrexate complex of

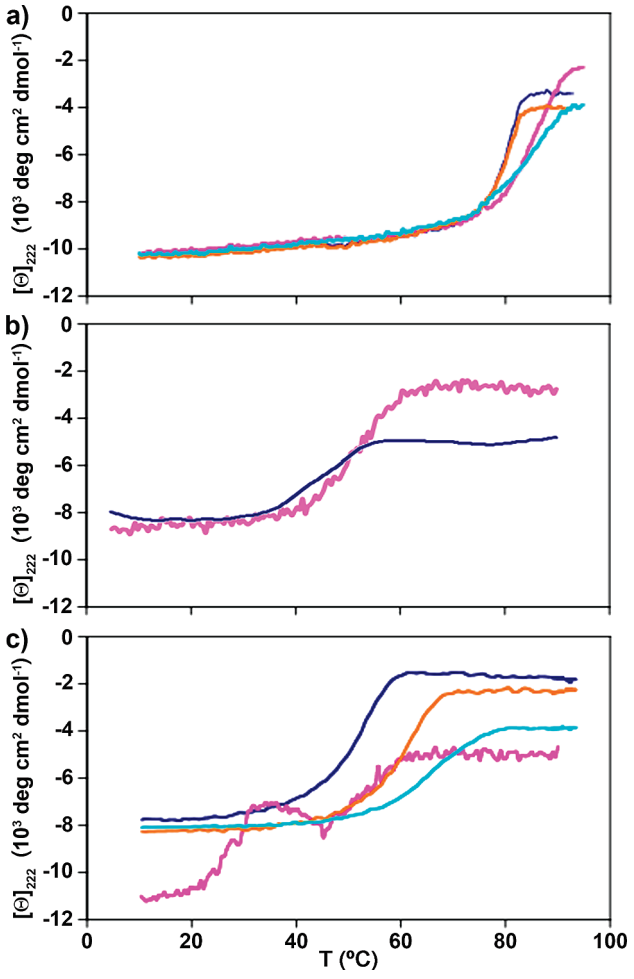

FIGURE 4: Thermal denaturation profiles of (a) TmDHFR, (b) TmDHFR-V126E, and (c) TmDHFR-V11D in 5 mM potassium phosphate (pH 7.0) (dark blue line), and 5 mM potassium phosphate (pH 7.0) containing 0.25% CHAPS (orange line), 10 μM MTX (pink line), or 10 μM MTX and 0.25% CHAPS (light blue line). Protein concentrations were 0.5 μM.

TmDHFR-V11D showed a double transition characterized by two individual midpoints at 28.4 ± 2.3 and 56.8 ± 3.0 °C (Figure 4 and Supporting Information). The molecular basis of this observation is unclear. A minor rearrangement of the protein fold at low temperature may be followed by the major unfolding reaction at elevated temperature. However, the reaction rate data presented below indicated monophasic kinetics for TmDHFR-V11D between 5 and 40 °C suggesting that any structural change around 28 °C did not affect the monomer dimer equilibrium or the kinetic properties of the mutant. Upon addition of CHAPS, single melting transitions characterized the thermal unfolding of apo-TmDHFR-V11D and its methotrexate complex with midpoints at 59.9 ± 0.8 and 65.5 ± 1.3 °C, respectively (Figure 4 and Supporting Information). The presence of CHAPS did not affect the melting temperature of wild-type TmDHFR (Supporting Information) suggesting that CHAPS had a stabilizing effect on TmDHFR-V11D.

The thermal stability of TmDHFR-V11D was also determined by following the loss of activity with time at two temperatures. At 40 °C in the absence of CHAPS, TmDHFR-V11D showed no measurable activity within 60 h (Figure 5). In the presence of CHAPS, although an initial 8 h plateau was observed in which 100% activity was maintained, rapid activity loss followed and the enzyme again showed no measurable activity after 60 h

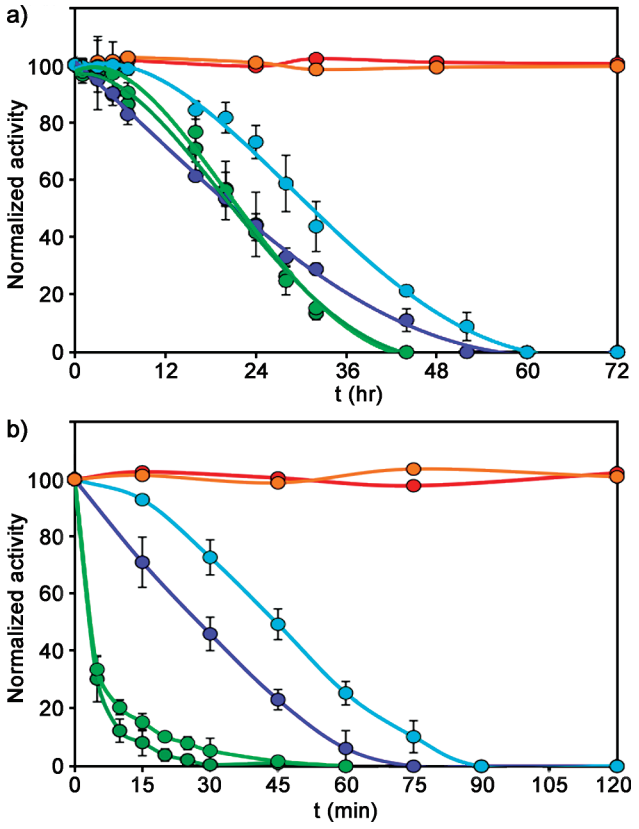

FIGURE 5: Loss of activity over time for TmDHFR (red line), TmDHFR + 0.25% CHAPS (orange line), TmDHFR-V11D (dark blue line), TmDHFR-V11D + 0.25% CHAPS (light blue line), EcDHFR (dark green line), and EcDHFR + 0.25% CHAPS (light green line) at (a) 40 °C and (b) 60 °C in 100 mM potassium phosphate buffer (pH 7.0) containing 100 mM NaCl. Error bars for the wild-type enzyme are obscured by the symbols. Activities were measured at 20 °C.

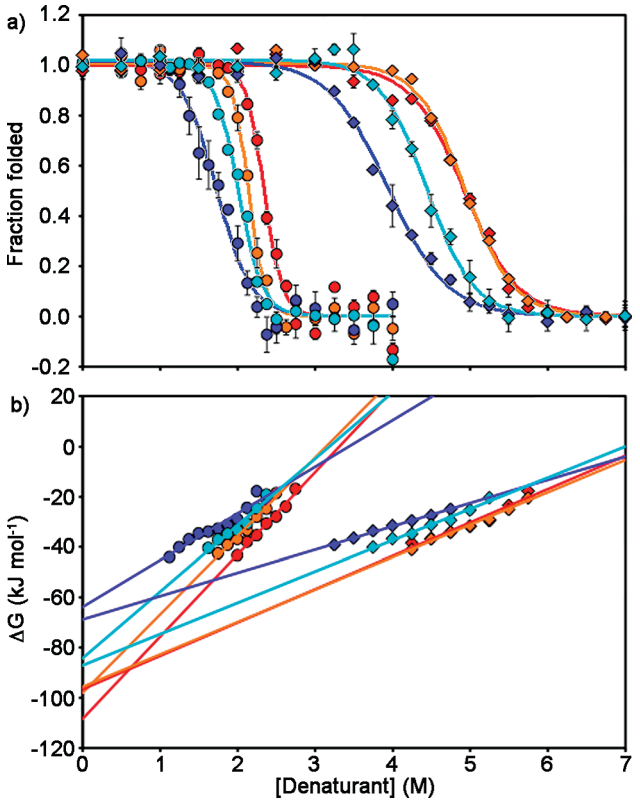

FIGURE 6: (a) Equilibrium unfolding transitions of 5 μM TmDHFR (red line), TmDHFR + 0.25% CHAPS (orange line), TmDHFR-V11D (dark blue line), and TmDHFR-V11D + 0.25% CHAPS (light blue line) at 20 °C. Denaturants are GdmHCl (circles) and urea (diamonds). Normalized signals of native fluorescence emission are plotted against denaturant concentration. (b) Linear extrapolation of ΔG in the transition region to zero denaturant concentration (error bars are obscured by the symbols).

despite the melting temperature being some 20 °C higher than the incubation temperature. Similarly, at 60 °C in the absence of CHAPS, TmDHFR-V11D was inactivated within 75 min (Figure 5), and the presence of CHAPS only slightly extended this time. In contrast, TmDHFR retained full activity even after five weeks at 40 °C, while at 60 °C only 50% activity loss was observed after 28 days in both the presence and absence of CHAPS (Figure 5). At 40 °C, EcDHFR in the presence or absence of CHAPS lost activity at a rate similar to TmDHFR-V11D in the absence of CHAPS. At 60 °C however, EcDHFR was inactivated more rapidly than TmDHFR-V11D (Figure 5). These measurements were not performed in the presence of ligands due to the instability of NADPH and H_2F over extended periods of time and at higher temperatures, and the prohibitive reduction in activity in the presence of methotrexate.

Equilibrium Unfolding Measurements. The stabilities of TmDHFR and TmDHFR-V11D at 20 °C were also investigated using equilibrium unfolding measurements in the presence of denaturants (Figure 6). The use of urea or guanidinium hydrochloride resulted in similar free energies of stabilization (Supporting Information) except for the wild-type enzyme, where ΔG was ~10 kJ mol^{-1} greater in guanidinium hydrochloride than in urea. The *m*-values, which measure the dependence of ΔG on denaturant concentration, increase as ΔG increases. They are generally lower for urea than for guanidinium hydrochloride, as has been found previously (*42*). The free energy of stabilization of TmDHFR was approximately 100 kJ mol^{-1}, while for TmDHFR-V11D this value was more than 30 kJ mol^{-1} lower. In the presence of CHAPS little difference in ΔG was seen for TmDHFR. However, the detergent raised the free energy of stabilization of TmDHFR-V11D to approximately 85 kJ mol^{-1} (Figure 6 and Supporting Information), consistent with the thermal stability studies (vide supra), which showed little difference in the thermal stability of TmDHFR in the presence of CHAPS, but a large increase in the melting temperature of TmDHFR-V11D. Even in the absence of CHAPS, the value of 67 kJ mol^{-1} for TmDHFR-V11D is almost three times higher than the value of 25 kJ mol^{-1} obtained for EcDHFR (*37*), showing that the monomer unit of TmDHFR is intrinsically more stable than the mesophilic enzyme. With the caveat that we are comparing the monomer of a mutant of TmDHFR to the dimer of the wild-type enzyme, it appears that dimerization provides significant stabilization allowing TmDHFR to operate at its physiological temperature.

Ligand Binding. To investigate the possibility that the presence of CHAPS could hinder the binding of ligands, tryptophan fluoresence emission spectra of TmDHFR and TmDHFR-V11D in the presence and absence of CHAPS were recorded with varying concentrations of NADPH, H_2F, and methotrexate. Emission spectra for both enzymes and the end points for titration with ligands were similar whether or not CHAPS was present (Figure 7). Since substoichiometric concentrations of ligands were used, dissociation constants were not determined. The intensity of the FRET emission from NADPH was increased in the presence of CHAPS, suggesting a change in the active site

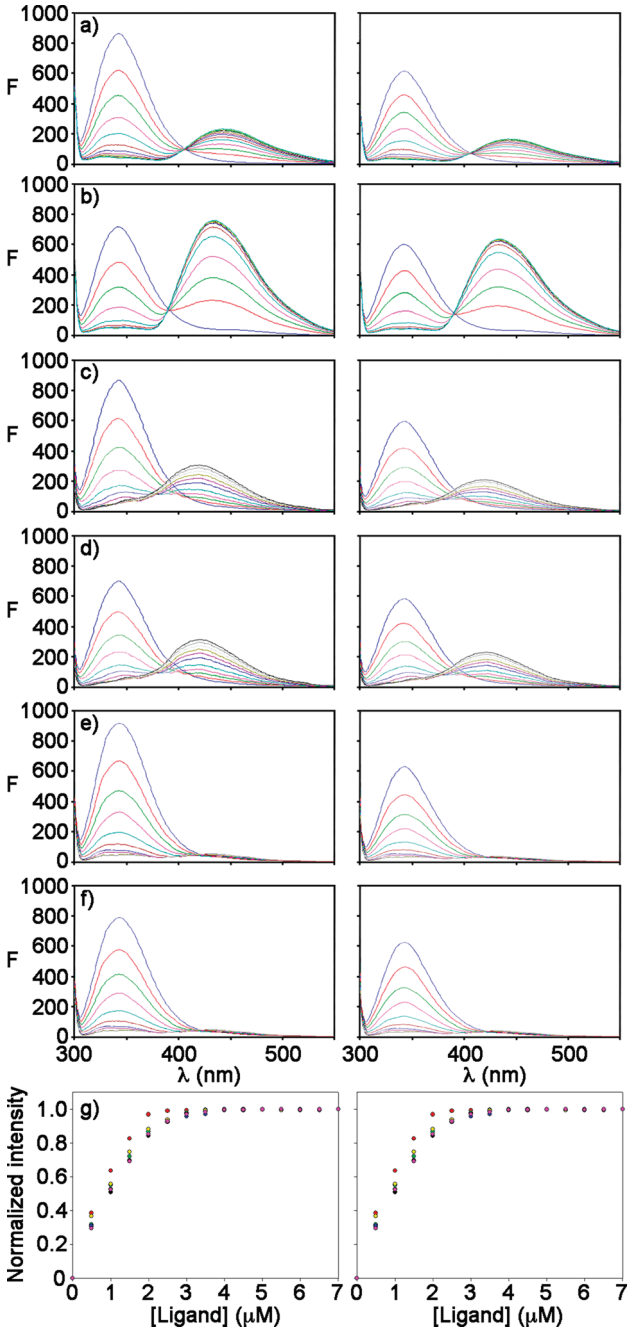

FIGURE 7: Fluorescence emission spectra following irradiation at 292 nm of 4 μM TmDHFR (left) and TmDHFR-V11D (right) alone (blue curve) and in the presence of 0.5 μM increments of (a) NADPH, (b) NADPH in the presence of 0.25% CHAPS, (c) dihydrofolate, (d) dihydrofolate in the presence of 0.25% CHAPS, (e) methotrexate, (f) methotrexate in the presence of 0.25% CHAPS, and (g) plots of normalized fluorescence intensity at 340 nm against ligand concentration, where black = NADPH, red = NADPH in the presence of 0.25% CHAPS, green = dihydrofolate, yellow = dihydrofolate in the presence of 0.25% CHAPS, blue = methotrexate and purple = methotrexate in the presence of 0.25% CHAPS.

geometry in the presence of the detergent, but this was observed for the wild-type enzyme as well as the mutant and hence cannot be attributed to dimerization. These results demonstrate both that TmDHFR-V11D is fully capable of binding ligands and that the presence of CHAPS does not inhibit ligand binding or partially denature the enzymes.

Structure and Stability of TmDHFR-V11D. The above results demonstrate that TmDHFR-V11D can be converted to a fully monomeric form by the addition of the detergent CHAPS. Despite having many of its properties altered in a similar manner to TmDHFR-V11D, TmDHFR-V126E remained a dimer under identical conditions. Val11 is found in a loop region toward the center of the dimer interface, whereas Val126 is located in a β-strand closer to the periphery. It is likely that the more central position of V11 is responsible for its greater influence on dimerization.

CD and ligand binding experiments indicated that the mutations to TmDHFR induce some structural changes to the enzyme and that the addition of CHAPS induces structural changes in TmDHFR-V11D. The detergent does however not appear to be partially denaturing the enzyme, as can also be seen from the effects of CHAPS on the melting temperature and the free energy of unfolding. In addition, TmDHFR-V11D is fully capable of binding ligands. Some structural differences are to be expected, as the insertion of an acidic residue into the hydrophobic dimer interface is likely to induce conformational changes that minimize unfavorable interactions. The presence of CHAPS considerably improves the stability of TmDHFR-V11D possibly due to the detergent binding to the exposed hydrophobic surface generated by the mutation.

Stabilization of TmDHFR-V11D by CHAPS complicated the analysis of the effect of dimerization on TmDHFR stability. In the absence of the detergent, monomeric TmDHFR-V11D had the same melting temperature as EcDHFR, but greater free energy of stabilization and longer inactivation times at elevated temperature. In the presence of CHAPS, the thermal stability of TmDHFR-V11D was significantly higher than that of EcDHFR. However, the isolated monomer unit of TmDHFR-V11D is likely to be destabilized due to its exposed hydrophobic surface, and hence the results in the presence of CHAPS may be a better comparison with naturally monomeric DHFRs. Under these conditions, the melting temperature of monomeric TmDHFR-V11D was some 10 °C higher than that of EcDHFR. The melting temperature of monomeric, CHAPS-stabilized TmDHFR-V11D was 20 °C lower than that of the wild-type dimer, while its free energy of stabilization is 15 kJ mol^{-1} lower. Even in the absence of CHAPS the combined evidence presented here shows that monomeric TmDHFR-V11D is intrinsically more stable than EcDHFR. This is most likely a consequence of a large number of energetically small, stabilizing interactions across the whole subunit as is typically observed for thermophilic enzymes. It is in agreement with the prediction made in a previous computational study that the monomer of TmDHFR should be of higher thermal stability than that of EcDHFR (*35*), at least within the limits imposed by the fact that a mutant of TmDHFR was analyzed.

In contrast to TmDHFR-V11D, the monomer−dimer equilibrium cannot be perturbed sufficiently in TmDHFR-V126E to allow the detection of a monomer under any of the conditions used here. Although the concentration of TmDHFR-V126E used for the thermal denaturation studies was below the lowest concentration used in the size exclusion chromatography experiments, it is unlikely that a significant concentration of monomer was present (vide supra). However, a comparison of the properties of TmDHFR-V126E and TmDHFR-V11D reveals that certain effects on the enzyme are a direct consequence of the mutation itself rather than of perturbation of the monomer−dimer equilibrium. We have included TmDHFR-V126E in these studies to distinguish between those effects in TmDHFR-V11D that are a simple consequence of the mutation

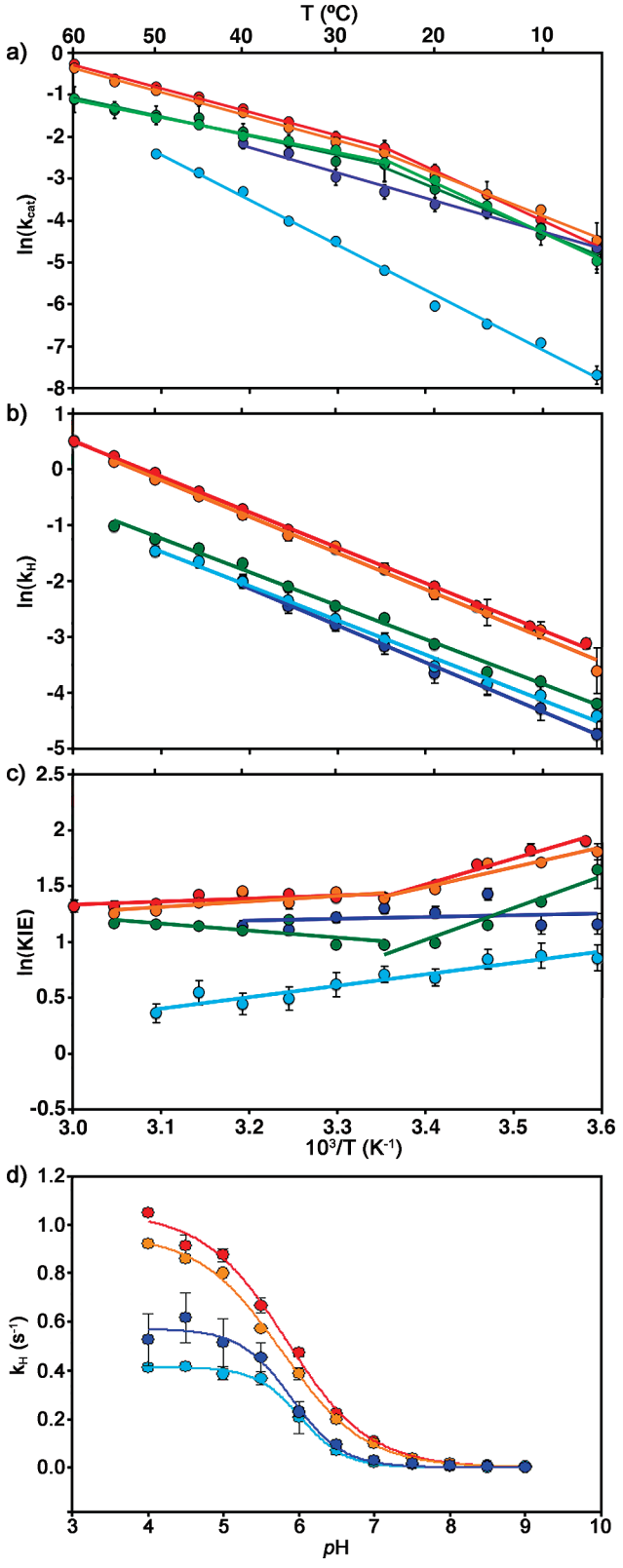

FIGURE 8: Arrhenius plots for (a) k_{cat} and (b) H-transfer, (c) logarithmic plot of the KIE, and (d) pH dependence of the H-transfer rate constant, of TmDHFR (red line), TmDHFR + 0.25% CHAPS (orange line), TmDHFR-V126E (dark green line), TmDHFR-V126E + 0.25% CHAPS (light green line), TmDHFR-V11D (dark blue line) and TmDHFR-V11D + 0.25% CHAPS (light blue line).

(and may therefore also be seen in TmDHFR-V126E), and those that result from monomerization (and hence are unique to TmDHFR-V11D).

Steady-State Kinetics. The steady-state rates of the reduction of H_2F by NADPH catalyzed by TmDHFR, TmDHFR-V126E, and TmDHFR-V11D were measured at pH 7 as a function of temperature (Figure 8A and Supporting Information). All K_m values were less than 1 μM (the high enzyme concentration required for the assay prevented the acquisition of more accurate values), further showing that the mutations and the presence of CHAPS do not significantly disrupt ligand binding. The turnover numbers (k_{cat}) for the wild-type enzyme increased from 0.010 ± 0.006 s^{-1} at 5 °C to 0.756 ± 0.034 s^{-1} at 60 °C. Although the three enzymes had similar turnover numbers at lower temperatures, the wild-type enzyme outperformed the two mutants with increasing temperatures. At 40 °C, the k_{cat} of 0.261 ± 0.007 s^{-1} for TmDHFR was more than twice that of TmDHFR-V11D (0.115 ± 0.014 s^{-1}), while TmDHFR-V126E displayed an intermediate k_{cat}. The Arrhenius plots (Figure 8A) showed biphasic behavior for both TmDHFR and TmDHFR-V126E, with k_{cat} showing a stronger dependence on temperature at temperatures below 25 °C in a manner similar to that observed for pre-steady-state deuteride transfer in the wild-type enzyme (*25*). The apparent activation energy for turnover in wild-type TmDHFR was 46.5 ± 1.1 kJ mol^{-1} above 25 °C and 80.5 ± 0.5 kJ mol^{-1} at lower temperatures. Activation energies for the mutants were similar (Supporting Information), except that monophasic behavior was observed for the k_{cat} of TmDHFR-V11D. Biphasic behavior for the k_{cat} of the wild-type enzyme shows that the structural transition which alters the mechanism of hydride transfer below 25 °C (as shown by the temperature dependence of the KIE rather than of hydride transfer itself) also has more wide-reaching effects on the enzyme, altering the kinetics of at least one physical step of the reaction as well as hydride transfer itself.

Since size exclusion chromatography had indicated that in 0.25% CHAPS TmDHFR-V11D was predominately monomeric even in the presence of substrate and cofactor, the steady-state rates were also measured in the presence of the detergent. CHAPS had little effect on the turnover numbers for the wild-type enzyme and for TmDHFR-V126E (Figure 8A and Supporting Information). The k_{cat} values for TmDHFR-V11D on the other hand were reduced up to 15-fold and the temperature dependence increased. The activation energy for turnover by TmDHFR-V11D was increased from 50.0 ± 2.6 kJ mol^{-1} in the absence of CHAPS to 89.0 ± 2.1 kJ mol^{-1} in its presence, showing that the barrier to reaction was greatly increased in the monomer. As had been observed in the absence of detergent, the Arrhenius plot for TmDHFR-V11D in 0.25% CHAPS showed no break point (Figure 8A). In all cases, k_{cat} was not affected by varying the concentration of enzyme between 0.1 and 2.5 μM, suggesting that the relative populations of monomer and dimer did not change.

Pre-Steady-State Kinetics. Since a step other than hydride transfer is partially rate limiting for TmDHFR (*17*), it was difficult to interpret the steady-state rates mechanistically and the temperature dependence of the rates of the actual chemical step was measured directly under pre-steady-state conditions. The first order rate constants of the hydride transfer step for TmDHFR, TmDHFR-V126E, and TmDHFR-V11D were determined from fluorescence resonance energy transfer experiments. In a typical experiment enzyme was incubated with NADPH, mixed with a large excess of substrate and the change in fluorescence followed as a function of time. All data was best fit to a single exponential as had been observed previously for wild-type TmDHFR (*25*).

The temperature dependence of the rate constants of TmDHFR, TmDHFR-V126E, and TmDHFR-V11D followed similar exponential increases (Figure 8B and Supporting Information). For TmDHFR, the rate constants of hydride transfer were at least two times larger than the steady-state turnover numbers over the whole temperature range, while for the two mutants hydride transfer and steady-state rate constants were similar. In contrast with those for k_{cat}, the Arrhenius plots for H-transfer catalyzed by TmDHFR and TmDHFR-V126E do not show biphasic behavior (Figure 8B). The biphasic behavior observed for k_{cat} therefore appears to be due to a physical step in the catalytic cycle having greater rate-limiting character below 25 °C. Hydride transfer catalyzed by TmDHFR-V126E and TmDHFR-V11D was generally approximately 4 times slower than for the wild-type enzyme. In comparison with the effect on the melting temperature, the V126E and V11D mutations caused a reduction in the catalytic activity of the enzyme irrespective of their effect on the monomer−dimer equilibrium.

Since ligand-bound TmDHFR-V11D was predominantly in the dimeric form at the relatively high concentrations of the pre-steady-state experiments (20 μM), the hydride transfer rates for TmDHFR and TmDHFR-V11D were also measured in 0.25% CHAPS, where the wild type retained its dimeric structure while the mutant existed predominantly as the monomer. The presence of the detergent did not significantly alter the rate of hydride transfer (Figure 8B). This is in contrast to the effect on k_{cat} for the TmDHFR-V11D catalyzed reaction, which was reduced by the detergent. Unlike the reaction in the absence of CHAPS, where TmDHFR-V11D is mainly dimeric, hydride transfer was not rate limiting in monomeric TmDHFR-V11D.

The temperature dependence of the rate of deuteride transfer catalyzed by TmDHFR and its two mutants was also determined (Supporting Information). TmDHFR-V126 showed a similar biphasic Arrhenius plot for deuteride transfer to the wild-type enzyme, with a breakpoint in the KIE at 25 °C (Figure 8C). In contrast, TmDHFR-V11D gave a monophasic Arrhenius plot for deuteride transfer and therefore a monophasic KIE, which was temperature independent over the entire experimental range. This suggests that in TmDHFR-V11D the active site remains in a similar "tunnelling-ready" configuration, and therefore gating motions do not dominate the reaction even at low temperatures. Given that TmDHFR-V126E retains biphasic behavior of the KIE, this suggests that highly specific interactions within the dimer interface of TmDHFR are involved. A similar effect has been seen in wild-type TmDHFR in the presence of polyol cosolvents (*43*), which was interpreted as being due to the cosolvent disrupting certain rigidifying interactions at the dimer interface. Disruption of these interactions − either by addition of polyol cosolvents or by the V11D mutation − reduces the reliance on gating motions. In contrast to the effect on hydride transfer, the presence of CHAPS caused a slight increase in the rate of deuteride transfer by TmDHFR-V11D, and an increase in the temperature dependence of the KIE.

Contrary to the computational prediction that the monomer of TmDHFR would have an increased activation energy for reaction (*34*), the activation energy of the reaction catalyzed by TmDHFR-V11D was not significantly increased in the presence of CHAPS (Supporting Information). In fact, the mutations themselves had little effect on the activation energy of the reaction. The reactions catalyzed by both TmDHFR-V126E and TmDHFR-V11D were found to have the same activation energies as the wild-type enzyme.

Effect of pH on TmDHFR-V11D Activity. To verify that the reduction in the rate constants for TmDHFR-V11D catalysis relative to the wild-type enzyme were not the consequence of a simple pK_a shift, and similarly that the presence of CHAPS did not influence the pK_a, rate constants for hydride transfer were determined at different values of pH (Figure 8D and Supporting Information). These experiments showed no difference in pK_a between wild-type TmDHFR (5.83 ± 0.06) and TmDHFR-V11D (5.91 ± 0.06) at 20 °C. These values are similar to those published previously for wild-type TmDHFR at 40 °C (*17*). The pK_a of the EcDHFR-catalyzed reaction is 6.5 (*36*), higher than that of the TmDHFR-catalyzed reaction. It has been shown computationally that the M20 loop of EcDHFR plays an important role in modulating the pK_a of the bound substrate (*44*). In TmDHFR the "M20 loop" is constrained by the dimer interface (*18*), and hence the pK_a of the reaction catalyzed by the monomeric TmDHFR-V11D might be expected to increase relative to the dimer. However, the presence of 0.25% CHAPS did not significantly affect the pK_a of either enzyme (5.77 ± 0.04 and 6.02 ± 0.03 for TmDHFR and TmDHFR-V11D, respectively). The mutation in the dimer interface and the presence of CHAPS clearly do not affect the ability of the enzyme to modulate the pK_a of bound substrate. Hence, dimerization alone is not the cause of the reduced pK_a of the TmDHFR catalyzed reaction when compared to EcDHFR.

The Effect of Monomerization on TmDHFR Catalysis. While dimerization contributes significantly to the stability of TmDHFR, the effect of quaternary structure on the catalytic activity is more subtle. Both the steady-state turnover and the hydride transfer were slower in TmDHFR-V11D than in the wild type. However, the rate of hydride transfer was not significantly affected by the presence of CHAPS and was similar to the rate of hydride transfer catalyzed by TmDHFR-V126E, suggesting that the mutations in the dimer interface had a more significant effect than the quaternary structure on the rate of reaction. Calculation of the rate constants by ensemble-averaged variational transition state theory with multidimensional tunnelling had predicted a reduction in the rates for hydride transfer by approximately 2 orders of magnitude in the hypothetical TmDHFR monomer relative to the native dimer (*34*). In contrast, the relatively small difference in the rates of hydride transfer catalyzed by dimeric and monomeric TmDHFR-V11D suggests that dimerization itself has only a rather small effect on the chemical step in TmDHFR catalysis. Correlated motions both within and between the subunits of TmDHFR have been observed computationally (*34*). From the experimental results presented here it appears that intersubunit motions are not critical to TmDHFR-catalyzed hydride transfer. On the other hand, dimerization greatly improves the steady-state turnover rate of TmDHFR-V11D (Figure 8), suggesting that intersubunit motions or at least intersubunit contacts are important for the physical steps in the TmDHFR reaction cycle. Therefore, the structural rigidity that results from dimerization is clearly not the cause of the reduced catalytic activity of the thermophilic TmDHFR dimer, in agreement with a recent computational study (*45*). In addition, the monomer of TmDHFR, in which the βFG loop and "M20 loop" are not constrained by the dimer interface, might also be expected to better modulate the pK_a of the substrate as seen in EcDHFR (*44*). However, the results presented here suggest that even when these loops have increased freedom, they are still unable to carry out the functions ascribed to them in EcDHFR. In a similar study of dimeric phosphoribosylanthranilate

isomerase (PRAI) from *T. maritima*, it was found that engineered monomeric variants had reduced thermostability but identical catalytic activities compared to the wild type enzyme (*46*). Unlike TmDHFR, the catalytic efficiency of the thermophilic PRAI was similar to that of its mesophilic *E. coli* homologue, most likely because the loop regions of PRAI involved in catalysis are different from those involved in dimerization, allowing that enzyme to form a thermostable dimer without compromising catalysis (*46*).

CONCLUSIONS

The increased stability of the monomer of TmDHFR-V11D relative to monomeric EcDHFR suggests that the subunits of wild-type TmDHFR are also optimized for stability, and hence the high resistance of TmDHFR to thermal and chemical denaturation is the result of both its quaternary structure and the intrinsic stability of its subunits. It is interesting to note in this context that the melting temperature of 65.5 °C for the methotrexate complex of fully monomeric TmDHFR-V11D in the presence of CHAPS is only slightly below that of the monomeric DHFR from the thermophile *Bacillus stearothermophilus* (BsDHFR), for which a thermal melting temperature that coincided with the optimal bacterial growth temperature of 65 °C has been reported (*47*). The thermal stability of the thermophilic BsDHFR may be the maximum that can be reached within the framework of the DHFR monomer and oligomerization may be necessary for activity at the temperatures optimal for growth of hyperthermophiles. Future structural work may therefore reveal that all hyperthermophilic DHFRs homologous to TmDHFR and EcDHFR rely on intersubunit contacts to achieve their high thermal stabilities.

Several recent studies have indicted that the flexibility of thermophilic enzymes is reduced at ambient temperatures, while the flexibilities of mesophilic and thermophilic enzymes are often comparable at their respective working temperatures (*48*−*51*). For DHFR, a correlation between flexibility and hydride transfer has been proposed (*47*), although recent computational results have contradicted this view (*45*), and it has also been shown experimentally that thermophilic BsDHFR has greater flexibility than mesophilic EcDHFR, suggesting instead that the thermophilic enzyme may better resist the larger fluctuation amplitudes at higher temperatures (*52*). In simulations, the βFG loop, which has been shown to be catalytically important in EcDHFR, exhibited reduced mobility in TmDHFR relative to that observed in EcDHFR, while in the hypothetical monomer of TmDHFR the flexibility of the residues in the βFG loop was increased (*35*). Rather than simply being a direct consequence of rigidity of the catalytically important loops resulting from dimerization, it seems that lower rates of the TmDHFR-catalyzed reaction relative to those of EcDHFR are due instead to modifications to these loops which allow dimerization but prevent their optimal function even when unconstrained by the dimer interface. The observation that TmDHFR-V11D was catalytically less efficient than the native dimer provides further evidence that it is not simply the mobility of these loop residues that controls the catalytic activity. Rather it may be the highly correlated nature of specific protein motions that controls catalysis, as had been suggested by covariance analysis where the catalytically less active monomer of TmDHFR was characterized by a reduction of the coupled motions relative to the native dimer (*34*). Such an interpretation is in agreement with the proposal from kinetic measurements that specific protein motions promote hydride transfer in TmDHFR catalysis, and with an environmentally coupled model of enzymatic hydrogen transfer (*25*).

ACKNOWLEDGMENT

We thank Dr. Jiayun Pang (University of Manchester) for stimulating discussions and Rhiannon Evans for providing Figure 1.

SUPPORTING INFORMATION AVAILABLE

Tables of size exclusion chromatography results, thermal melting temperatures, equilibrium unfolding data, and kinetic data. This material is available free of charge via the Internet at http://pubs.acs.org.

REFERENCES

(1) Blakley, R. L. (1984) Folates and Pterins , Wiley, New York.
(2) Sawaya, M. R., and Kraut, J. (1997) Loop and subdomain movements in the mechanism of *Escherichia coli* dihydrofolate reductase: Crystallographic evidence. *Biochemistry 36*, 586–603.
(3) Rajagopalan, P. T. R., Lutz, S., and Benkovic, S. J. (2002) Coupling interactions of distal residues enhance dihydrofolate reductase catalysis: Mutational effects on hydride transfer rates. *Biochemistry 41*, 12618–12628.
(4) Boehr, D. D., McElheny, D., Dyson, H. J., and Wright, P. E. (2006) The dynamic energy landscape of dihydrofolate reductase catalysis. *Science 313*, 1638–1642.
(5) McElheny, D., Schnell, J. R., Lansing, J. C., Dyson, H. J., and Wright, P. E. (2005) Defining the role of active-site loop fluctuations in dihydrofolate reductase catalysis. *Proc. Natl. Acad. Sci. U.S.A. 102*, 5032–5037.
(6) Venkitakrishnan, R. P., Zaborowski, E., McElheny, D., Benkovic, S. J., Dyson, H. J., and Wright, P. E. (2004) Conformational changes in the active site loops of dihydrofolate reductase during the catalytic cycle. *Biochemistry 43*, 16046–16055.
(7) Schnell, J. R., Dyson, H. J., and Wright, P. E. (2004) Effect of cofactor binding and loop conformation on side chain methyl dynamics in dihydrofolate reductase. *Biochemistry 43*, 374–383.
(8) Osborne, M. J., Schnell, J., Benkovic, S. J., Dyson, H. J., and Wright, P. E. (2001) Backbone dynamics in dihydrofolate reductase complexes: Role of loop flexibility in the catalytic mechanism. *Biochemistry 40*, 9846–9859.
(9) Epstein, D. M., Benkovic, S. J., and Wright, P. E. (1995) Dynamics of the dihydrofolate reductase folate complex - catalytic sites and regions known to undergo conformational change exhibit diverse dynamical features. *Biochemistry 34*, 11037–11048.
(10) Cameron, C. E., and Benkovic, S. J. (1997) Evidence for a functional role of the dynamics of glycine-121 of *Escherichia coli* dihydrofolate reductase obtained from kinetic analysis of a site-directed mutant. *Biochemistry 36*, 15792–15800.
(11) Radkiewicz, J. L., and Brooks, C. L. (2000) Protein dynamics in enzymatic catalysis: Exploration of dihydrofolate reductase. *J. Am. Chem. Soc. 122*, 225–231.
(12) Agarwal, P. K., Billeter, S. R., Rajagopalan, P. T. R., Benkovic, S. J., and Hammes-Schiffer, S. (2002) Network of coupled promoting motions in enzyme catalysis. *Proc. Natl. Acad. Sci. U.S.A. 99*, 2794–2799.
(13) Benkovic, S. J., and Hammes-Schiffer, S. (2003) A perspective on enzyme catalysis. *Science 301*, 1196–1202.
(14) Wilquet, V., Gaspar, J. A., van de Lande, M., van de Casteele, M., Legrain, C., Meiering, E. M., and Glansdorff, N. (1998) Purification and characterization of recombinant *Thermotoga maritima* dihydrofolate reductase. *Eur. J. Biochem. 255*, 628–637.
(15) Dams, T., Bohm, G., Auerbach, G., Bader, G., Schurig, H., and Jaenicke, R. (1998) Homo-dimeric recombinant dihydrofolate reductase from *Thermotoga maritima* shows extreme intrinsic stability. *Biol. Chem. 379*, 367–371.
(16) Dams, T., and Jaenicke, R. (1999) Stability and folding of dihydrofolate reductase from the hyperthermophilic bacterium *Thermotoga maritima*. *Biochemistry 38*, 9169–9178.
(17) Maglia, G., Javed, M. H., and Allemann, R. K. (2003) Hydride transfer during catalysis by dihydrofolate reductase from *Thermotoga maritima*. *Biochem. J. 374*, 529–535.
(18) Dams, T., Auerbach, G., Bader, G., Jacob, U., Ploom, T., Huber, R., and Jaenicke, R. (2000) The crystal structure of dihydrofolate

reductase from *Thermotoga maritima*: Molecular features of thermostability. *J. Mol. Biol. 297*, 659–672.
(19) Basran, J., Sutcliffe, M. J., and Scrutton, N. S. (1999) Enzymatic H-transfer requires vibration-driven extreme tunneling. *Biochemistry 38*, 3218–3222.
(20) Kohen, A., Cannio, R., Bartolucci, S., and Klinman, J. P. (1999) Enzyme dynamics and hydrogen tunnelling in a thermophilic alcohol dehydrogenase. *Nature 399*, 496–499.
(21) Harris, R. J., Meskys, R., Sutcliffe, M. J., and Scrutton, N. S. (2000) Kinetic studies of the mechanism of carbon-hydrogen bond breakage by the heterotetrameric sarcosine oxidase of *Arthrobacter* sp 1-IN. *Biochemistry 39*, 1189–1198.
(22) Francisco, W. A., Knapp, M. J., Blackburn, N. J., and Klinman, J. P. (2002) Hydrogen tunneling in peptidylglycine alpha-hydroxylating monooxygenase. *J. Am. Chem. Soc. 124*, 8194–8195.
(23) Knapp, M. J., and Klinman, J. P. (2002) Environmentally coupled hydrogen tunneling - Linking catalysis to dynamics. *Eur. J. Biochem. 269*, 3113–3121.
(24) Basran, J., Harris, R. J., Sutcliffe, M. J., and Scrutton, N. S. (2003) H-tunneling in the multiple H-transfers of the catalytic cycle of morphinone reductase and in the reductive half-reaction of the homoligous Pentaerythritol tetranitrate reductase. *J. Biol. Chem. 278*, 43973–43982.
(25) Maglia, G., and Allemann, R. K. (2003) Evidence for environmentally coupled hydrogen tunneling during dihydrofolate reductase catalysis. *J. Am. Chem. Soc. 125*, 13372–13373.
(26) Swanwick, R. S., Maglia, G., Tey, L. H., and Allemann, R. K. (2006) Coupling of protein motions and hydrogen transfer during catalysis by *Escherichia coli* dihydrofolate reductase. *Biochem. J. 394*, 259–265.
(27) Agrawal, N., Hong, B. Y., Mihai, C., and Kohen, A. (2004) Vibrationally enhanced hydrogen tunneling in the *Escherichia coli* thymidylate synthase catalyzed reaction. *Biochemistry 43*, 1998–2006.
(28) Sikorski, R. S., Wang, L., Markham, K. A., Rajagopalan, P. T. R., Benkovic, S. J., and Kohen, A. (2004) Tunneling and coupled motion in the *Escherichia coli* dihydrofolate reductase catalysis. *J. Am. Chem. Soc. 126*, 4778–4779.
(29) Masgrau, L., Roujeinikova, A., Johannissen, L. O., Hothi, P., Basran, J., Ranaghan, K. E., Mulholland, A. J., Sutcliffe, M. J., Scrutton, N. S., and Leys, D. (2006) Atomic description of an enzyme reaction dominated by proton tunneling. *Science 312*, 237–241.
(30) Allemann, R. K., Evans, R. M., Tey, L. H., Maglia, G., Pang, J. Y., Rodriguez, R., Shrimpton, P. J., and Swanwick, R. S. (2006) Protein motions during catalysis by dihydrofolate reductases. *Phil. Trans. R. Soc. B 361*, 1317–1321.
(31) Hay, S., Pang, J. Y., Monaghan, P. J., Wang, X., Evans, R. M., Sutcliffe, M. J., Allemann, R. K., and Scrutton, N. S. (2008) Secondary kinetic isotope effects as probes of environmentally-coupled enzymatic hydrogen tunneling reactions. *ChemPhysChem 9*, 1536–1539.
(32) Kuznetsov, A. M., and Ulstrup, J. (1999) Proton and hydrogen atom tunnelling in hydrolytic and redox enzyme catalysis. *Can. J. Chem. 77*, 1085–1096.
(33) Knapp, M. J., Seebeck, F. P., and Klinman, J. P. (2001) Steric control of oxygenation regiochemistry in soybean lipoxygenase-1. *J. Am. Chem. Soc. 123*, 2931–2932.
(34) Pang, J. Y., Pu, J. Z., Gao, J. L., Truhlar, D. G., and Allemann, R. K. (2006) Hydride transfer reaction catalyzed by hyperthermophilic dihydrofolate reductase is dominated by quantum mechanical tunneling and is promoted by both inter- and intramonomeric correlated motions. *J. Am. Chem. Soc. 128*, 8015–8023.
(35) Pang, J. Y., and Allemann, R. K. (2007) Molecular dynamics simulation of thermal unfolding of *Thermotoga maritima* DHFR. *Phys. Chem. Chem. Phys. 9*, 711–718.
(36) Fierke, C. A., Johnson, K. A., and Benkovic, S. J. (1987) Construction and evaluation of the kinetic scheme associated with dihydrofolate reductase from *Escherichia coli*. *Biochemistry 26*, 4085–4092.
(37) Iwakura, M., Jones, B. E., Luo, J. B., and Matthews, C. R. (1995) A strategy for testing the suitability of cysteine replacements in dihydrofolate reductase from *Escherichia coli*. *J. Biochem. 117*, 480–488.
(38) Swanwick, R. S., Daines, A. M., Tey, L. H., Flitsch, S. L., and Allemann, R. K. (2005) Increased thermal stability of site-selectively glycosylated dihydrofolate reductase. *ChemBioChem 6*, 1338–1340.
(39) Walsh, K. A. J., Daniel, R. M., and Morgan, H. W. (1983) A Soluble NADH dehydrogenase (NADH-ferricyanide oxidoreductase) from *Thermus aquaticus* strain T351. *Biochem. J. 209*, 427–433.
(40) Dams, T., and Jaenicke, R. (2001) Dihydrofolate reductase from *Thermotoga maritima*. *Methods Enzymol. 331*, 305–317.
(41) Swanwick, R. S., Shrimpton, P. J., and Allemann, R. K. (2004) Pivotal role of Gly121 in dihydrofolate reductase from *E. coli*: Altered structure of a mutant enzyme may form basis of diminished catalytic performance. *Biochemistry 43*, 4119–4127.
(42) Myers, J. K., Pace, C. N., and Scholtz, J. M. (1995) Denaturant m-values and heat capacity changes − relation to changes in accessible surface areas of protein unfolding. *Protein Sci. 4*, 2138–2148.
(43) Loveridge, E. J., Evans, R. M., and Allemann, R. K. (2008) Solvent effects on environmentally coupled hydrogen tunnelling during catalysis by dihydrofolate reductase from *Thermotoga maritima*. *Chem.—Eur. J. 14*, 10782–10788.
(44) Rod, T. H., and Brooks, C. L. (2003) How dihydrofolate reductase facilitates protonation of dihydrofolate. *J. Am. Chem. Soc. 125*, 8718–8719.
(45) Roca, M., Liu, H., Messer, B., and Warshel, A. (2007) On the relationship between thermal stability and catalytic power of enzymes. *Biochemistry 46*, 15076–15088.
(46) Thoma, R., Hennig, M., Sterner, R., and Kirschner, K. (2000) Structure and function of mutationally generated monomers of dimeric phosphoribosylanthranilate isomerase from *Thermotoga maritima*. *Struct. Fold. Des. 8*, 265–276.
(47) Kim, H. S., Damo, S. M., Lee, S. Y., Wemmer, D., and Klinman, J. P. (2005) Structure and hydride transfer mechanism of a moderate thermophilic dihydrofolate reductase from *Bacillus stearothermophilus* and comparison to its mesophilic and hyperthermophilic homologues. *Biochemistry 44*, 11428–11439.
(48) Zavodszky, P., Kardos, J., Svinger, A., and Petsko, G. A. (1998) Adjustment of conformational flexibility is a key event in the thermal adaptation of protein. *Proc. Natl. Acad. Sci. U.S.A. 95*, 7406–7411.
(49) Kohen, A., and Klinman, J. P. (2000) Protein flexibility correlates with degree of hydrogen tunneling in thermophilic and mesophilic alcohol dehydrogenase. *J. Am. Chem. Soc. 122*, 10738–10739.
(50) Henzler-Wildman, K., Wolf-Watz, M., Thai, V., and Kern, D. (2004) The role of fast-timescale dynamics in enzyme catalysis. *Protein Sci. 13*, 104–104.
(51) Wolf-Watz, M., Thai, V., Henzler-Wildman, K., Hadjipavlou, G., Eisenmesser, E. Z., and Kern, D. (2004) Linkage between dynamics and catalysis in a thermophilic-mesophilic enzyme pair. *Nat. Struct. Mol. Biol. 11*, 945–949.
(52) Meinhold, L., Clement, D., Tehei, M., Daniel, R., Finney, J. L., and Smith, J. C. (2008) Protein dynamics and stability: The distribution of atomic fluctuations in thermophilic and mesophilic dihydrofolate reductase derived using elastic incoherent neutron scattering. *Biophys. J. 94*, 4812–4818.